THE JOURNAL OF BIOLOGICAL CHEMISTRY VOL. 286, NO. 45, pp. 39403–39416, November 11, 2011
Printed in the U.S.A.

Sorting Nexin 27 Protein Regulates Trafficking of a p21-activated Kinase (PAK) Interacting Exchange Factor (β-Pix)-G Protein-coupled Receptor Kinase Interacting Protein (GIT) Complex via a PDZ Domain Interaction*

Received for publication, May 13, 2011, and in revised form, September 16, 2011 Published, JBC Papers in Press, September 18, 2011, DOI 10.1074/jbc.M111.260802

Julie L. Valdes[‡], Jingrong Tang[‡], Mark I. McDermott[‡], Jean-Cheng Kuo[‡§], Seth P. Zimmerman[‡], Stephen M. Wincovitch[‡], Clare M. Waterman[‡], Sharon L. Milgram[‡], and Martin P. Playford[‡1]

From the [‡]Cell Biology and Physiology Center, NHLBI, National Institutes of Health, Bethesda, Maryland 20982 and the [§]Institute of Biochemistry and Molecular Biology, National Yang-Ming University, Taipei 112, Taiwan

Background: Sorting Nexin 27 regulates intracellular trafficking of proteins through the endosomal system.
Results: An interaction between SNX27 and the guanine nucleotide exchange factor β-Pix in complex with Git family proteins is identified.
Conclusion: Cells lacking SNX27 have decreased cell motility, which we propose to be due to β-Pix intracellular trafficking defects.
Significance: The results and model proposed have implications for recruitment/activation of p21-activated kinase (PAK) or Rho GTPases at focal adhesions.

Sorting nexin 27 (SNX27) is a 62-kDa protein localized to early endosomes and known to regulate the intracellular trafficking of ion channels and receptors. In addition to a PX domain, SNX27 is the only sorting family member that contains a PDZ domain. To identify novel SNX27-PDZ binding partners, we performed a proteomic screen in mouse principal kidney cortical collecting duct cells using a GST-SNX27 fusion construct as bait. We found that β-Pix (p21-activated kinase-interactive exchange factor), a guanine nucleotide exchange factor for the Rho family of small GTPases known to regulate cell motility directly interacted with SNX27. The association of β-Pix and SNX27 is specific for β-Pix isoforms terminating in the type-1 PDZ binding motif (ETNL). In the same screen we also identified Git1/2 as a potential SNX27 interacting protein. The interaction between SNX27 and Git1/2 is indirect and mediated by β-Pix. Furthermore, we show recruitment of the β-Pix·Git complex to endosomal sites in a SNX27-dependent manner. Finally, migration assays revealed that depletion of SNX27 from HeLa and mouse principal kidney cortical collecting duct cells significantly decreases cell motility. We propose a model by which SNX27 regulates trafficking of β-Pix to focal adhesions and thereby influences cell motility.

The endocytic system is a series of compartments that determine the fate of intracellular protein cargo. Such cargo is commonly delivered from the plasma membrane to endosomal compartments where a number of trafficking decisions can be made. For example, the protein may be delivered to lysosomes and degraded or recycled to the cell surface (1). However, it has recently been proposed that endosomes may also serve as a platform for protein-protein interactions to regulate a range of cellular processes such as migration, polarity, and cytokinesis (1, 2)

The sorting nexin family of proteins is characterized by the presence of phosphoinositide-binding PX domains, which direct sorting nexins to phospholipid-rich cell membranes (3). In addition to the PX domain, many sorting nexins contain other known protein-protein interaction domains. These include the Src homology 3 domain in SNX9 and -18 and others as well as the regulator of G-protein signaling domain in SNX13, -14, and -25 (3, 4). The relatively large number of proteins in the sorting nexin family along with the diverse array of protein interaction domains present in each suggests multiple roles for this family during endosomal trafficking (3).

SNX27 is unique in the sorting nexin family in containing a postsynaptic density protein-95, discs large, zona occludens 1 (PDZ) domain (3, 5). PDZ domains are one of the largest domain families involved in protein-protein interactions. They primarily function by interacting with short amino acid motifs at the C termini of target proteins (6). To date, the PDZ domain of SNX27 has been shown to interact with enzymes, receptors, and ion channels (7–10).

Multiple studies have localized SNX27 to the early endosome (7, 9, 11). The PX domain is responsible for SNX27 localization (7, 9). The PDZ domain of SNX27 has been proposed to traffic a growing list of proteins via endosomal-mediated pathways. For example, Lunn *et al.* (9) have proposed that SNX27 regulates Kir3 potassium channel endocytosis and lysosomal degradation. More recently, data by Lauffer *et al.* (7) suggest a role for SNX27 in the recycling of β_2-adrenoreceptors from the early endosome to the plasma membrane. In this study we demonstrate intracellular trafficking of a novel protein complex via an interaction with SNX27. In a proteomic screen using the SNX27-PDZ domain as bait, we identified the proteins

* This work was supported, in whole or in part, by a National Institutes of Health grant from the NHLBI.
[1] To whom correspondence should be addressed: Bldg. 10, Rm. 6N256, National Institutes of Health, 9000 Rockville Pike, Bethesda, MD 20892. Tel.: 301-451-4364; Fax: 301-402-1443; E-mail: playfordmp@nhlbi.nih.gov.

β-Pix (PAK-interacting exchange factor)[2] and Git (G-protein receptor kinase interacting target) as novel SNX27 interacting proteins.

β-Pix (also known as Cool-1 and ARHGEF7) was first identified as a binding partner to the PAK family of Cdc42/Rac1-activated kinases (12). In the same article, β-Pix was identified in focal complexes and demonstrated to be involved in PAK recruitment to these sites (12). β-Pix has also been shown to target the Rac1 GTPase to focal adhesions (13). Both Rac and PAK compete for the Src homology 3 domain of β-Pix (13). In the absence of PAK, elevated levels of Rac1 in complex with β-Pix were observed, a condition that led to increased cell spreading (13). Hence, interplay between β-Pix, Rac1, and PAK may modulate cell adhesion and motility.

Regulation of cell motility by β-Pix might also involve the Git family of proteins (14). Like β-Pix, two members of this family, Git1 and Git2, localize to focal complexes (15, 16). Git proteins contain an amino-terminal ARF GTPase-activating protein domain, three ankyrin repeats, a Spa-2 homology domain (SHD), a coiled-coil domain, and a carboxyl-terminal binding site for paxillin (14). A number of binding partners have been shown to interact with each domain. For example, the SHD domain has been found to interact with β-Pix, which enables Git to interact with PAK, Rac, and Cdc42 (15). Several studies have demonstrated that the β-Pix-Git interaction is constitutive and may exist in complexes in excess of 1 MDa. Recent data has also demonstrated the existence of an unusually stable heteropentameric complex with dimeric Git interacting with trimeric Pix (17–19). The interaction between Git and β-Pix may be weakened by phosphorylation of β-Pix at Tyr^{442} (20). Under these conditions, the Git-paxillin interaction is facilitated and proposed to disassemble focal adhesions (20). Git proteins have also been observed in endosomes (21, 22). Location of Git proteins to these sites is mediated by the first of the three amino-terminal ankyrin repeats (21). Here, Git proteins were proposed to mediate membrane recycling between endosomes and the plasma membrane where nascent focal contacts form (21). Taken together, the involvement of β-Pix-Git in cell migration is complex and involves phosphorylation events, transient protein-protein interactions, and intracellular trafficking.

Here we present evidence of a SNX27·β-Pix·Git complex. The interaction between SNX27 and β-Pix is direct, with β-Pix as the central component of this trimeric complex. We also show that SNX27 is responsible for recruitment of the β-Pix·Git complex to endosomal sites and propose that, during cell motility, the β-Pix·Git complex recycles between the endocytotic system and focal contact sites.

EXPERIMENTAL PROCEDURES

Materials—A polyclonal antibody to a GST-SNX27 fusion (amino acids 1–265) was generated by Lampire Biological Laboratories (Pipersville, PA) and Primm Biotech (Cambridge, MA). Monoclonal antibodies against fusion proteins tagged with c-Myc (clone 9E10), HA (clone HA-11), and GFP (clone JL8) were purchased from Abcam (Cambridge, MA), Covance (Princeton, NJ), and Clontech (Mountain View, CA), respectively. Anti-paxillin, anti-Git1, anti-Git2, and anti-β-Pix monoclonal antibodies were purchased from BD Biosciences. Anti-β-Pix and Git1 polyclonal antibodies were purchased from Millipore (Billerica, MA) and Cell Signaling (Beverly, MA), respectively. Anti-α-tubulin monoclonal antibody was purchased from Sigma. β-Pix/ARHGEF7 variant 1 and 3 plasmid DNA molecules (catalog numbers sc117668 and sc318985) were purchased from Origene (Rockville, MD). Git1 and Git2 plasmid DNA molecules were purchase from Open Biosytems (Huntsville, AL). All chemicals were purchased from Sigma, unless otherwise stated.

Molecular Biology—The cDNA sequence of human SNX27b was amplified by PCR and cloned into the BamHI and XhoI sites of pCMV-Myc (Invitrogen), PET28c (Novagen EMD Chemicals, Gibbstown, NJ), and pEGFP (Clontech). SNX27b mPDZ point mutation was generated using the QuikChange® Site-directed Mutagenesis kit (Stratagene, La Jolla, CA) following the manufacturer's instructions using primers 5′-caagtccgagtccggcggcggcggcaacgtgcggggccaag-3′ and 5′-cttggccccgcacgttgccgccgccgccggactcggacttg-3′. A SNX27b mutant lacking the PDZ domain was generated by inverse PCR using primers 5′-P-gtacctcctcatgaggcagataacc-3′ and 5′-P-ggcgcagtggagcccagaccccc-3′. PCR-based cloning was also used to clone Git1 into pEYFPc1 (Clontech) and β-Pix into pCMV-HA (Invitrogen) or mCherry-c1 (Clontech). DNA primer sequences and protocols for these procedures and all others herein are available upon request. All constructs were sequenced to ensure the absence of undesired secondary mutations (Macrogen, Rockville, MD).

Cell Culture and Transfection—Mouse primary kidney cortical collecting duct (mpkCCD) clone 3 cells were kindly provided by Mark Knepper (NHLBI, National Institutes of Health). MpkCCD and HeLa cells were maintained in high glucose, Dulbecco's modified Eagle's medium (Invitrogen) supplemented with 10% fetal bovine serum (Sigma) in humidified chambers with 5% CO_2 at 37 °C. NIH3T3 cells were obtained from the American Tissue Culture Collection (ATCC, Manassas, VA) and maintained in high glucose, Dulbecco's modified Eagle's medium (Invitrogen) supplemented with 10% normal calf serum (Invitrogen). MpkCCD cells were transfected using Lipofectamine LTX reagent including Plus reagent (Invitrogen) using the manufacturer's recommended instructions. Similarly, HeLa and NIH3T3 cells were transfected using FuGENE HD (Roche). Cells were typically analyzed for protein expression using Western blotting or immunofluorescence 24–48 h post-transfection. Transfection of siRNA molecules in NIH3T3 or mpkCCD cells was performed with Oligofectamine™ (Invitrogen) using a reverse transfection protocol as per the manufacturer's instructions. Murine-specific β-Pix/ARHGEF7 siRNA molecules were purchased from Dharmacon (number L063023-01-0010).

Stable shRNA expressing cells were generated using an inducible lentiviral shRNA system (pINDUCER10) and selected with puromycin (23). A set of shRNA sequences specific for SNX27 were purchased from Open Biosystems (num-

[2] The abbreviations used are: β-Pix, PAK-interacting exchange factor; Git, G-protein receptor kinase interacting target; SHD, Spa-2 homology domain; mpkCCD, mouse primary kidney cortical collecting duct; PAK, p21-activated kinase.

ber RHS4531-NM_030918). The clone IDs for each shRNA are shRNA#2 V3LHS_412022, shRNA#5 V3LHS_383895, shRNA#6 V3LHS_383896, shRNA#7 V2LHS_273547, shRNA#8 V2LHS_237898, and shRNA#9 V3LHS_383899, respectively. Clone number 5 may be used to target human or mouse SNX27. These sequences were subcloned from pGIPZ to pINDUCER10 with MluI and XhoI digests. An identical method was used to prepare control (firefly luciferase) lentivirus. Lentiviral supernatants were generated by transient transfection of 293T cells using FuGENE HD (Roche Applied Science). HeLa and mpkCCD stable cell lines were generated by lentiviral transduction as described (23). shRNA expression on puromycin-resistant clones were routinely induced with 1 μg/ml of doxycycline for 72–96 h prior to experimental analysis.

In Vitro Translation—To investigate whether the interaction of SNX27 with β-Pix is direct, β-Pix variant 1, variant 3, or variant 1 with the PDZ binding motif deleted (ΔETNL) were subcloned (SalI-NotI) into pBlueScript SK (Stratagene). One microgram of each construct was translated using ([^{35}S]Met) and the TnT® T7 Quick-coupled Transcription/Translation system (Promega, Madison, WI) following the manufacturer's instructions. Ninety percent of the translated product was diluted in NETN buffer (125 mM NaCl, 1 mM EDTA, 20 mM Tris-Cl, pH 8.1, 0.5% Nonidet P-40, 10% glycerol) containing protease inhibitors. The diluted translated product was tumbled with 2 μg of the indicated GST fusion proteins conjugated to Sepharose beads for 1 h at 4 °C. The beads were washed 5 times, boiled in sample buffer, and run on an SDS-PAGE gel. Ten percent of the translated product was used as input. The gel was stained with Coomassie Blue, dried, and exposed to film.

Expression of Recombinant Proteins in Bacteria—The PDZ domain of human SNX27 was cloned by PCR into the BamHI-EcoRI site of pGEX2T using the following primers: 5′-CATGGATCCCCGCGGGTCGTGCGCATC-3′ and 5′-CATGAATTCCAGATAACACTGTCAAGATCAATTC-3′ and transformed into BL21(DE3) cells (Stratagene). SNX27-PDZ fusion protein expression was induced with 0.1 mM isopropyl β-D-thiogalactopyranoside for 3 h at room temperature. The bacterial cells were lysed by sonication for 1 min in PBS and proteins were solubilized in Triton X-100 diluted to 1% final volume. Fusion proteins were collected by incubation at 4 °C with glutathione-Sepharose 4B beads (GE Healthcare). The fusion proteins were quantified by SDS-PAGE and staining with Coomassie Blue.

Protein Analysis—For GST pulldown experiments, mpkCCD, HeLa, or NIH3T3 cells were lysed in binding buffer 150 (BB150: 50 mM Tris, pH 7.6, 150 mM NaCl, 0.2% CHAPS, 10 mM EDTA) plus Complete™ protease inhibitor mixture (Roche Applied Science). GST pulldowns were typically performed using ~500 μg of protein and 10–20 μg of fusion protein immobilized on glutathione beads for 3 h at 4 °C. The beads were washed three times in lysis buffer, and boiled in sample buffer. For immunoprecipitation experiments, cells were lysed in 0.1% Triton X-100 lysis buffer (0.1% Triton X-100, 0.3 M sucrose, 50 mM Tris·HCl, pH 7.5, 100 mM KCl, 1 mM $CaCl_2$, 2.5 mM $MgCl_2$) containing Complete™ protease inhibitors. The protein concentration was determined using the bicinchoninic acid assay (Pierce Biotechnology, Rockford, IL). Immunoprecipitations were routinely performed using 1–2 mg of protein and 2–5 μg of purified SNX27 antibody or Myc polyclonal antibody conjugated to Sepharose beads and incubated at 4 °C (Sigma). SNX27-immune complexes were precipitated using protein A-Sepharose, washed twice with lysis buffer, and boiled in Laemmli sample buffer. Immune complexes and proteins bound to GST fusion proteins were analyzed by Western blotting and detected using the indicated primary antibodies incubated at 1:500 (Git1/2) or 1:1000 (SNX27) followed by secondary antibodies conjugated to IRdye 780 nm (rabbit) or IRdye 680 nm (mouse) (Licor, Lincoln NE) at 1:10,000 dilution. Detection of Myc tag by Western blotting was performed using the 9E10 monoclonal antibody used at 1:5,000 dilution followed by a secondary antibody conjugated to horseradish peroxidase and detected by enhanced chemiluminescence (1:10,000; Millipore).

Mass Spectrometry—To identify novel proteins bound to SNX27-PDZ, samples were run on an SDS-polyacrylamide gel, and the bands were visualized by silver staining. Protein identification by mass spectrometry was done in the NHLBI proteomics core, at the National Institutes of Health. The band of interest was excised and digested with trypsin at a 1:50 enzyme/substrate ratio. The dried tryptic digest was analyzed on an LTQ-Orbitrap XL (Thermo-Fisher Scientific LLC) interfaced with an Eksigent nano-LC one-dimensional plus system (Eksigent Technologies LLC, Dublin, CA) using CID fragmentation. Samples were loaded onto an Agilent Zorbax 300SB-C18 trap column at a flow rate of 5 μl/min for 10 min, and then separated on a reversed-phase PicoFrit analytical column (New Objective, Woburn, MA) using a 40-min linear gradient of 2–40% acetonitrile in 0.1% formic acid at a flow rate of 300 nl/min. LTQ-Orbitrap XL settings were as follows: spray voltage, 1.5 kV; full MS mass range, m/z 200 to 2000. The LTQ-Orbitrap XL was operated in a data-dependent mode; *i.e.* MS1 in the ion trap, scan for precursor ions followed by six data-dependent MS2 scans for precursor ions above a threshold ion count of 2000 with collision energy of 35%.

Data Base Search—The raw file generated from the LTQ-Orbitrap XL was analyzed using Proteome Discoverer version 1.2 software (Thermo-Fisher Scientific, LLC) using our six-processor Mascot cluster search engine at the NIH (biospec.nih.gov, version 2.3). The following search criteria was set to: data base, Sprot (Swiss Institute of Bioinformatics); taxonomy, *Mus musculus* (mouse); enzyme, trypsin; miscleavages, 2; fixed modification, carbamidomethylation (+57 Da); variable modification, methionine oxidation (+16 Da); deamidation (N,Q), acetyl (protein N-terminal); MS peptide tolerance as 1.0 Da; MS/MS tolerance as 0.8 Da. Protein identifications were based on 2 or more unique peptides with a false discovery rate set to 0.01.

Immunofluorescence—HeLa or NIH3T3 cells were plated on fibronectin-coated glass coverslips (coated overnight, 4 °C; 10 μg/ml in phosphate-buffered saline) and transfected as indicated. Cells were fixed with 4% paraformaldehyde for 10 min, permeabilized with 0.25% Triton X-100 for 5 min, and incubated in blocking buffer (2% bovine serum albumin (BSA) in PBS) for 1 h at 37 °C. The fixed coverslips were incubated with

primary antibodies at the following concentrations (HA, 1:1000; Myc, 1:1000; polyclonal β-Pix, 1:100; monoclonal Git1 or -2, 1:100) in blocking buffer overnight at 4 °C. Coverslips were washed extensively with PBS and incubated with the indicated secondary antibodies (Alexa Fluor 488, 568, 594, or 647 nm, Invitrogen) used at 1:1000 dilution in blocking buffer for 1 h at 37 °C. Following further washing with PBS, coverslips were mounted using FluorSave™ (Calbiochem). Wide-field images were collected using a Personal DeltaVision system (Applied Precision Inc., Issaquah, WA) mounted on an inverted Olympus IX71 microscope with an oil immersion PlanApo N ×60/1.42 objective lens. All images were acquired using a CoolSNAP ES2 CCD camera with 2 × 2 binning and a 512 × 512 pixels imaging field. All images were deconvolved using an iterative constrained method with 10 cycles of medium noise filtering in Applied Precision's SoftWoRx software package version 4.0.0. TIRF microscopy and quantification of endogenous β-Pix at focal contact sites was performed as previously described (24). To analyze the changes of focal abundance of endogenous β-Pix in HeLa cells expressing SNX27 WT and SNX27 ΔPDZ, double-labeled immunofluorescence images were quantified in the following manner: images of immunolocalized paxillin and β-Pix were median filtered with a 3-pixel square kernel and background flattened with a 13-pixel square kernel. Next, regions of the cell were manually selected to include all segmented paxillin-marked focal adhesions. The regions were transferred to the β-Pix immunofluorescence image of the same cell. The mean β-Pix intensity of the focal adhesion in SNX27 WT or SNX27 ΔPDZ-expressing cells was divided by the mean intensity of β-Pix at focal adhesions in GFP-expressing cells (control) to generate the fractional focal adhesion immunofluorescence signal change ± S.D. as reported in the figures. Statistical significance ($p < 0.05$) was measured by a Student's *t* test between control and SNX27 WT-expressing cells or control and SNX27 ΔPDZ-expressing cells. The velocity of individual HeLa or mpkCCD cells was measured using Image-Pro Plus version 7.0 (Media Cybernetics, Bethesda, MD).

RESULTS

Identification of a Novel SNX27 Binding Partner—As a first step in the identification of novel binding partners to the PDZ domain of SNX27, we generated a recombinant GST fusion protein containing this domain. GST-PDZ or GST recombinant proteins were incubated with mpkCCD cell lysates or with lysis buffer alone (Fig. 1*a*). After washing, proteins bound to GST beads were separated by SDS-PAGE and identified by Coomassie Blue staining (Fig. 1*a*). Two proteins of approximate molecular mass of 80 and 90 kDa were both readily stained with Coomassie and uniquely present in pulldowns of GST-PDZ from kidney cell lysates (Fig. 1*a*, *column 4*). The two protein bands were excised, subjected to in-gel trypsin digest, and the identity of each determined by matrix-assisted laser desorption/ionization mass spectrometry (MALDI-MS/MS). The protein of 80 kDa was identified as β-Pix/ARHGEF7 (49% peptide coverage) (Fig. 1*b*). Two members of the Git family were present in the 90-kDa band; they were identified as Git1 and Git2 (62.8 and 46.5% peptide coverage), respectively (Fig. 1*b*).

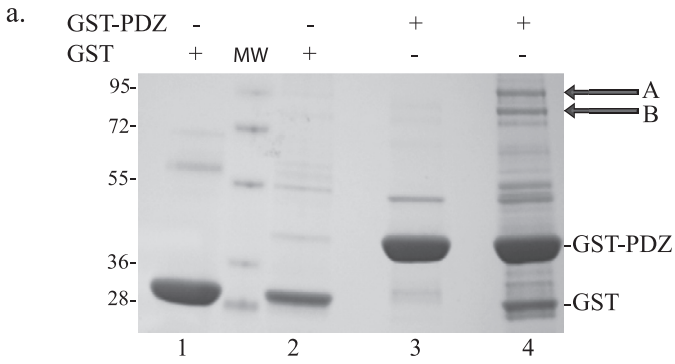

b.

Band	I.D.	Peptides	% Coverage
A	Git1/Git2	33/21	62.8 /46.5
B	β-Pix/ARHGEF	35	49.0

FIGURE 1. **Identification of β-Pix and Git1/2 as potential SNX27 PDZ binding partners.** *a,* 10 mg of mpkCCD cell extracts (*lanes 2* and *4*) or lysis buffer (*lanes 1* and *3*) were incubated with 50 μg of GST-SNX27 PDZ (*3* and *4*) or GST controls (*1* and *2*) for 2 h at 4 °C. After washing, bound proteins were separated by SDS-PAGE and identified by Coomassie staining. Bands unique to *lane 4* (*A* and *B*) were excised, in gel digested with trypsin, and analyzed by mass spectrometry, as described under "Experimental Procedures." *b,* the most abundant protein species present in *band A* was identified as Git1 and Git2 and in *band B* was β-Pix. *MW*, molecular weight marker.

Validation That SNX27 Binds β-Pix—To validate the finding that SNX27 can bind β-Pix, we performed GST pulldown and immunoprecipitation experiments (Fig. 2). Lysates from mpkCCD and HeLa cells were incubated with GST alone, GST-PDZ, or a mutant GST-PDZ protein where a conserved GΦGΦ (GYGF in SNX27) is mutated to GGGG (mPDZ). This conserved hydrophobic sequence is found within a loop connecting strands βA and βB and is responsible for binding C-terminal peptide ligands on binding partners (25). GST beads were washed and bound β-Pix was identified by Western blotting. Whereas β-Pix did not bind to GST or GST-mPDZ, it was associated with GST-PDZ in both mpkCCD and HeLa cells (Fig. 2*a*). To further verify that the PDZ domain on SNX27 is involved in β-Pix interaction, a series of Myc-tagged SNX27 constructs were expressed in mpkCCD cells (Fig. 2*b*). Along with full-length SNX27 (wild type), mPDZ or deletion mutants lacking the PDZ (ΔPDZ) or FERM/RA (ΔFERM) domains were engineered into full-length SNX27 (Fig. 2*b*). Expressed Myc-SNX27 proteins were isolated by immunoprecipitation and the presence of β-Pix was identified by Western blot (Fig. 2*b*). β-Pix co-immunoprecipitated with Myc-SNX27 WT and Myc-SNX27 ΔFERM immunoprecipitates, but Myc-SNX27 mPDZ and Myc-SNX27 ΔPDZ mutants were defective for β-Pix binding (Fig. 2*b*). We also detected the presence of a lower molecular weight β-Pix species in protein lysates but not Myc pulldowns. This may be a previously reported shorter form of β-Pix (26). Of additional note was the reproducible observation of increased β-Pix binding to Myc-ΔFERM/RA, suggesting that this domain may negatively regulate protein-protein interactions with SNX27 PDZ. In conclusion, we have confirmed the novel interaction between SNX27 and β-Pix and demonstrated

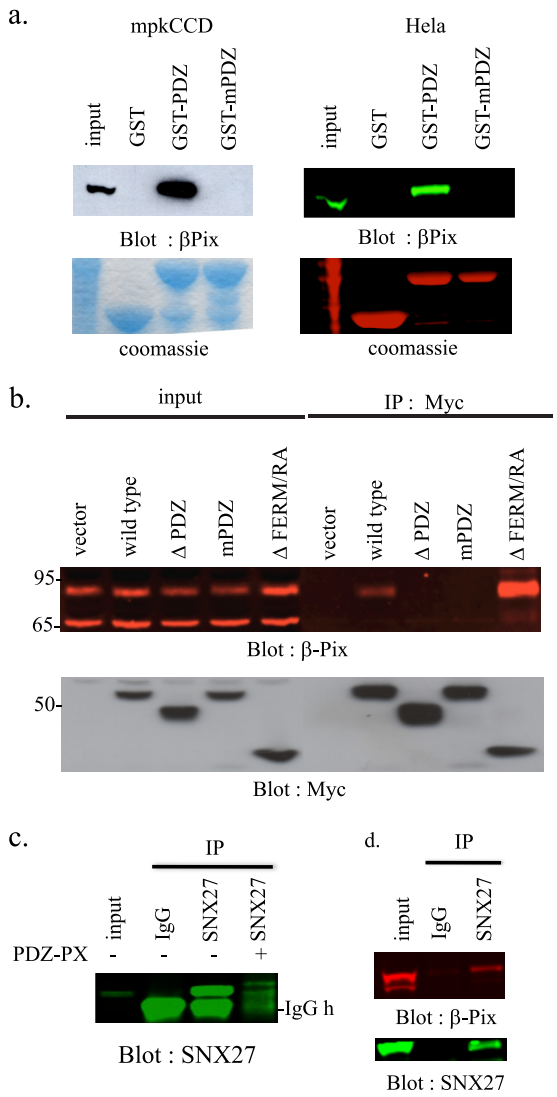

FIGURE 2. **Validation of β-Pix as a novel PDZ-dependent SNX27 binding partner.** *a*, 500 μg of mpkCCD (*i*) or HeLa (*ii*) cell lysates were incubated with 10 μg of GST or GST fusion proteins containing the SNX27 wild type (*GST-PDZ*) or mutant (*GST-mPDZ*) PDZ domain known to abolish C-terminal peptide ligand interactions. After washing, bound β-Pix was detected by Western blotting. 50 μg of lysate were loaded as control for Western blotting. Equal GST loading was verified by Coomassie staining. *b*, mpkCCD cells were transiently transfected with empty Myc-tagged vector or plasmids containing Myc fusion proteins of the indicated SNX27 sequences. After a 48-h incubation, the expressed fusion proteins were immunoprecipitated from cell lysates using a Myc antibody, and the immune complexes were blotted for β-Pix (*top*) or Myc (*bottom*). *c*, NIH3T3 cell lysates (1 mg) were incubated with a SNX27 polyclonal antibody (1 μg), preimmune serum, or SNX27 polyclonal antibody preincubated with the SNX27 PDZ-PX domain (2 μg). Immune complexes were collected using protein A-Sepharose. Immunoprecipitated SNX27 was detected by Western blotting. *d*, NIH3T3 cell lysates (10 mg) were incubated with a SNX27 polyclonal antibody or preimmune serum (10 μl). Immune complexes were collected using protein A-Sepharose. Bound β-Pix was detected by Western blotting. 50 μg of cell lysate was run as input control.

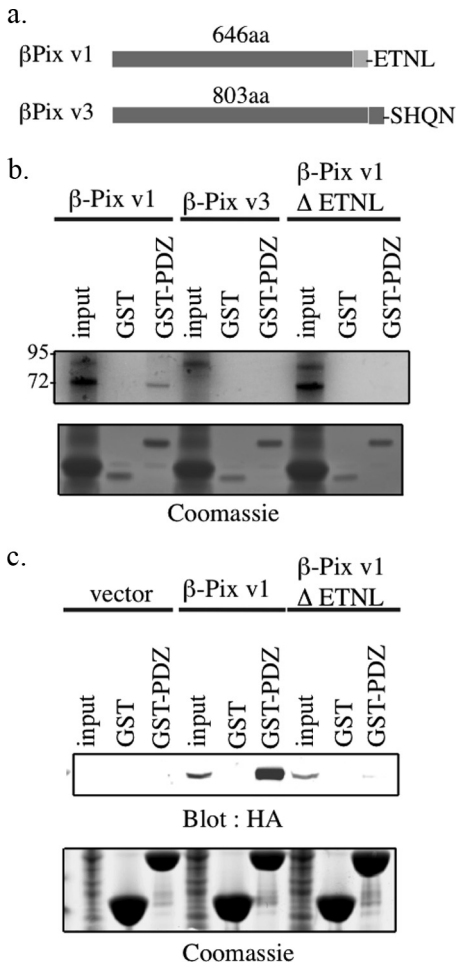

FIGURE 3. **The SNX27-β-Pix interaction is direct and specific for the β-Pix isoform containing the carboxyl-terminal PDZ binding motif.** *a*, schematic diagram of two variants of β-Pix. Variant 1 (β1-Pix) is shorter and contains a C-terminal type I PDZ binding motif sequence (ETNL). Variant 3 (β2-Pix) is longer and lacks this binding motif (SHQN). *b*, 1 μg of cDNAs of β-Pix variant 1, variant 3, or a mutant variant 1 lacking the C-terminal PDZ binding motif (ΔETNL) were translated in the presence of [^{35}S]methionine. The translated product was incubated with GST or GST fusion protein encoding the PDZ domain of SNX27 for 1 h at 4 °C. The beads were washed, and bound translated product was separated by SDS-PAGE. Detection of bound product was revealed by autoradiography. Twenty percent of the translated product was used as input control. *c*, mpkCCD cells were transiently transfected with empty HA-tagged vector or plasmids containing HA fusion proteins of the indicated β-Pix sequences. After 48 h incubation, the mpkCCD cell lysates were incubated with GST or a GST-SNX27 PDZ. Expressed fusion protein bound to GST/GST-PDZ was identified by Western blotting using an HA-specific antibody (*top*). Equal GST loading was confirmed by Coomassie staining (*bottom*). 20 μg of protein lysate was used as input.

that the association between the two proteins involves the PDZ domain of SNX27.

To determine whether the SNX27-β-Pix interaction occurs at normal physiological levels, endogenous SNX27 was immunoprecipitated from NIH3T3 cell lysate using SNX27 polyclonal antiserum. First, as a test for specificity, this antibody (1 μg) was preincubated in the presence or absence of competing SNX27-PDZ-PX domain (2 μg) and the immunocomplexes were analyzed by Western blotting for SNX27 (Fig. 2*c*). SNX27 was readily detected in SNX27 immunocomplexes, but diminished when the antibody was preincubated with PDZ-PX and absent in preimmune controls (Fig. 2*c*). SNX27-containing immune complexes were subsequently analyzed by Western blotting using a β-Pix monoclonal antibody. Endogenous β-Pix was detected in the SNX27 immune complex but not in the preimmune control (Fig. 2*d*).

β-Pix has been reported to exist in several isoforms (26). β1-Pix contains a putative carboxyl-terminal type I PDZ binding (ETNL) region, which is absent in β2-Pix (SHQN) (Fig. 3*a*). β1-Pix may exist in two additional variants, which differ only in

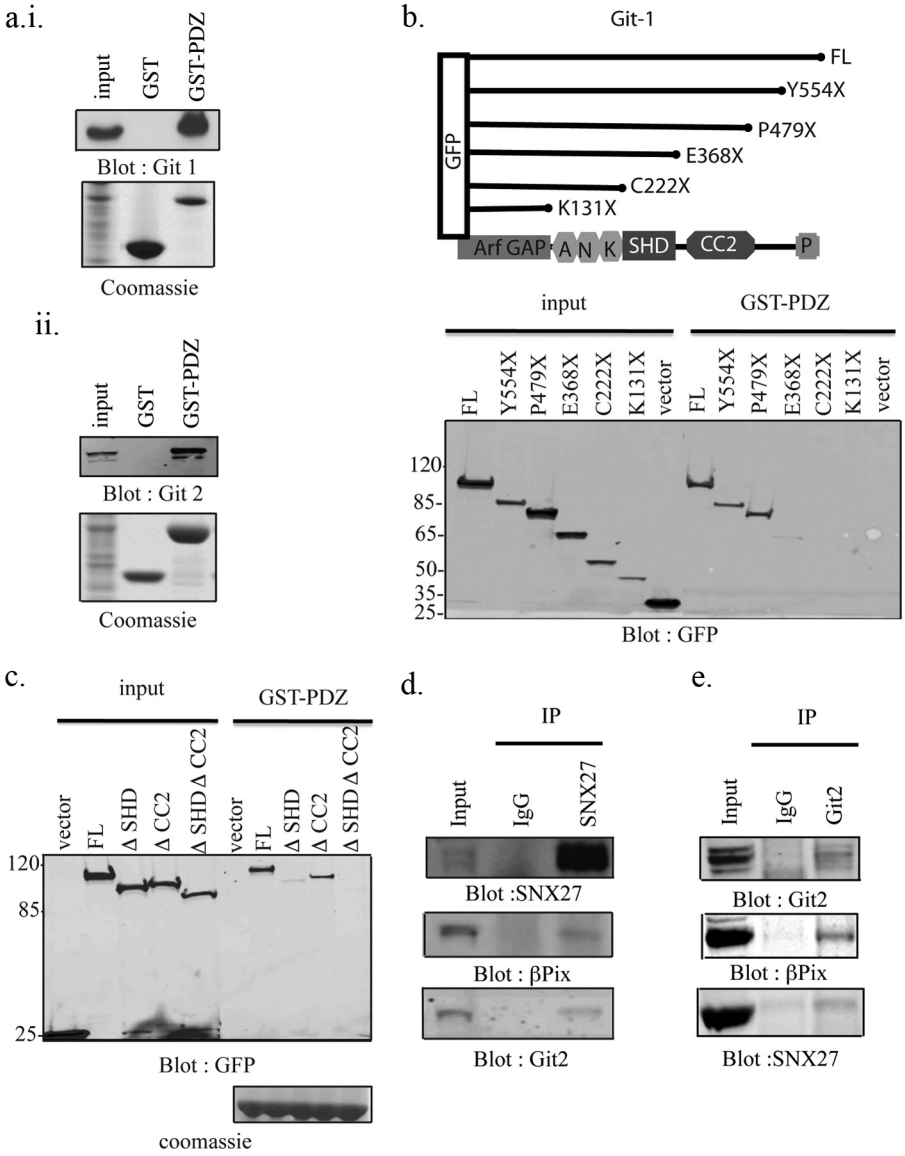

FIGURE 4. **Validation of Git1/2 as a SNX27 binding partner.** *a*, 500 μg of mpkCCD cell lysates were incubated with 10 μg of GST or GST fusion proteins containing the SNX27 (GST-PDZ) PDZ domain. After washing, bound Git1 (*i*) or Git2 (*ii*) were detected by Western blotting. 50 μg of lysate was loaded as control for Western blotting. Equal GST loading was verified by Coomassie staining. *b*, schematic diagram of GFP-tagged wild type and deletion constructs of Git1 (*top*). MpkCCD cells were transiently transfected with empty GFP-tagged vector or plasmids containing GFP fusion proteins of the indicated Git1 sequences. After a 48-h incubation, 500 μg of cell lysates were incubated with 10 μg of GST-SNX27 PDZ for 2 h at 4 °C. The GST-bound complexes were washed and separated by SDS-PAGE. GST-PDZ-bound Git1 fusion protein was identified by Western blotting using a GFP antibody (*bottom*). *c*, mpkCCD cells were transiently transfected with empty GFP-tagged vector or plasmids containing GFP fusion proteins of the indicated Git1 wild type (*FL*) or deletion mutants lacking the Spa-2 homology domain (Δ*SHD*) or second putative coiled-coil sequence (Δ*CC2*), or both. After a 48-h incubation, 500 μg of cell lysates were incubated with 10 μg of GST-SNX27 PDZ for 2 h at 4 °C. The GST-bound complexes were washed and separated by SDS-PAGE. GST-PDZ-bound Git1 fusion protein was identified by Western blotting using a GFP antibody (*top*). Equal loading was verified with Coomassie staining (*bottom*). *d*, NIH3T3 cell lysates (10 mg) were incubated with a SNX27 polyclonal antibody or preimmune serum (10 μl). Immune complexes were collected using protein A-Sepharose. The presence of immunoprecipitated SNX27 (*top*), immunocomplex bound β-Pix (*middle*), or Git2 (*bottom*) were detected by Western blotting using the respective antibodies. 50 μg of cell lysate was run as input control. *e*, NIH3T3 cell lysates (5 mg) were incubated with a Git2 monoclonal antibody or purified mouse IgG (5 μg). Immune complexes were collected using protein G-Sepharose. The presence of immunoprecipitated Git2 (*top*), immunocomplex bound β-Pix (*middle*), or SNX27 (*bottom*) was detected by Western blotting using respective antibodies. 50 μg of cell lysate was run as input control.

5′ and 3′ untranslated regions. The β1-Pix isoform used herein is termed variant 1 (NCBI accession number NP_003890). β2-Pix may exist in three different variants, which differ by alternative splicing of internal exons. The longest isoform (803 amino acids) of β2-Pix, which we term variant 3 (NCBI accession number NP_01106983.1), is used in this study.

Given that β1-Pix/variant 1 and β2-Pix/variant 3 differ at the C termini we proposed that the interaction between SNX27 and β-Pix might be isoform dependent. To this end, *in vitro* translated β-Pix variants 1 and 3 and a variant 1 with four carboxyl-terminal residues deleted (ΔETNL) were incubated with GST alone or GST-PDZ (Fig. 3*b*). β1-Pix variant 1 clearly associated with GST-PDZ but β1-Pix variant 3 and variant 1 ΔETNL did not (Fig. 3*b*). Furthermore, no binding of β1-Pix variants to GST control beads was observed (Fig. 3*b*). Similarly, when expressed in mpkCCD cells, HA-tagged β-Pix variant 1 but not v1ΔENTL associated with GST-PDZ (Fig. 3*c*). Taken together, the interaction between SNX27 and β1-Pix is direct and spe-

cific for the β1-Pix variant containing the carboxyl-terminal type I PDZ binding motif.

Validation That SNX27 Binds Git1/2—Having confirmed the SNX27-β-Pix interaction, we turned our attention to the mechanism by which SNX27 interacts with Git1/2 (Fig. 4). Lysates from mpkCCD cells were incubated with GST or GST-PDZ proteins. Both Git1 (*i*) or Git2 (*ii*) were readily found in GST-PDZ, but not GST bead complexes (Fig. 4*a*). Both members of the Git family lack putative carboxyl-terminal PDZ binding motifs (Git1, EKKQ; Git2, ENNN). However, multiple studies have demonstrated a robust interaction between β-Pix and Git, which led to the hypothesis that SNX27, Pix, and Git may form a tripartite complex (27). To identify the binding site on Git1 for SNX27, a series of GFP-tagged Git1 truncation constructs were generated and the ability of each to bind to GST-PDZ was tested (Fig. 4*b*). GFP-Git FL (wild type Git1), Y554X (lacking the paxillin binding site), P479X,E368X (lacking the largest coiled coil region and putative heterodimerization sequences), C222X (lacking the β-Pix binding site), K131X (lacking the ANK repeats), and GFP alone were expressed in mpkCCD cells (14). Western blotting revealed that the GFP-tagged constructs were expressed to similar levels (Fig. 4*b*). GFP-Git FL and GFP-Git Y554X or Git P479X mutants were readily detected in GST·PDZ bead complexes, but the interaction between GST·PDZ and E368X was greatly diminished (Fig. 4*b*). Binding of shorter Git1 mutants or GFP to GST·PDZ was not observed (Fig. 4*b*).

Git1 Cys^{222}-Pro^{479} contains the SHD and CC2 domains. To demonstrate the requirement of SHD and CC2 for SNX binding, single and double deletion mutants were engineered in GFP-Git1 FL (Fig. 4*c*). GFP-Git ΔCC2 was still detected in GST·PDZ complexes, albeit diminished in comparison with GFP-Git FL. GFP-Git ΔSHD was almost completely defective for GST-PDZ binding (Fig. 4*c*). GFP-Git double deletion mutant (ΔSHD ΔCC2) was completely absent in GST·PDZ bead complexes (Fig. 4*c*). Finally, we demonstrated that physiological levels of β-Pix and Git2 could be detected in SNX27, but not control immunoprecipitates (Fig. 4*d*). Similarly, a small amount of SNX27 was detected in Git2, but not control immunoprecipitates (Fig. 4*e*). In conclusion, the data are consistent with a hypothesis that β-Pix, SNX27, and Git form a tripartite complex with β-Pix as the central component, which binds simultaneously to the SHD domain on Git and the PDZ domain on SNX27.

To further test this hypothesis, GFP-Git FL or ΔSHD were co-expressed with HA-β-Pix variant 1 or varient 1 ΔENTL and incubated with GST·PDZ (Fig. 5*a*). We detected a basal level of GFP-Git in the GST·PDZ complexes, an interaction likely to be mediated by endogenous β-Pix (Fig. 5*a*, *top row*). However, the proportion of bound GFP-Git in GST·PDZ complexes was dramatically elevated in cells where HA-β-Pix variant 1, but not HA-β-Pix variant 1 ΔETNL, was co-expressed (Fig. 5*a*). Levels of PDZ bound β-Pix variant 1 were not elevated beyond control levels in cells expressing β-Pix binding-deficient GFP-GitΔSHD (Fig. 5*a*).

To further demonstrate that β-Pix is the fulcrum of the Git·β-Pix·SNX27 complex we used an RNA interference strategy to deplete endogenous β-Pix in mpkCCD (Fig. 5*b*) and

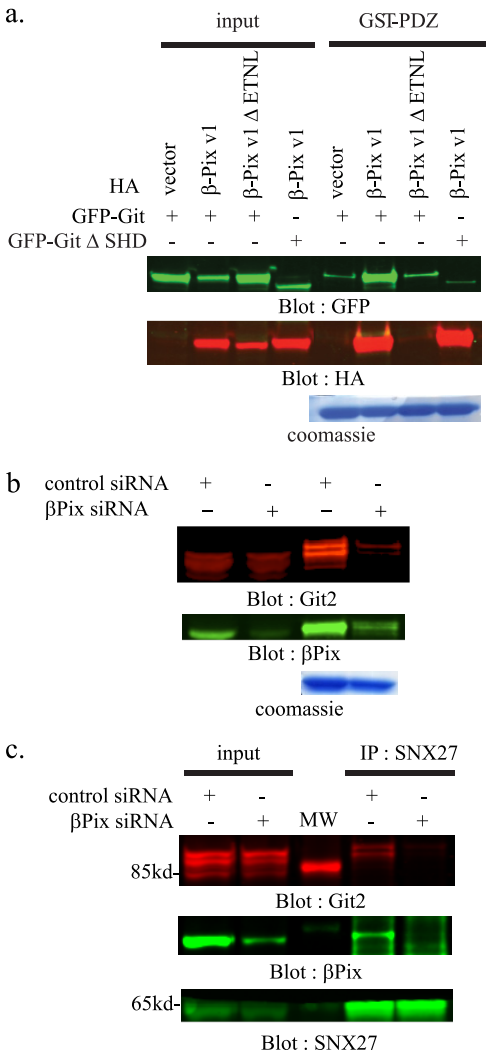

FIGURE 5. **β-Pix is essential for the SNX27-Git interaction.** *a,* the indicated HA-tagged β-Pix expression constructs were co-expressed with GFP-tagged wild type Git1 or Git1 lacking the Spa-2 homology domain (Δ*SHD*) in mpkCCD cells. After a 48-h incubation, cell lysates (500 μg) were incubated with 10 μg of GST-SNX27 PDZ for 2 h at 4 °C. The GST-PDZ bound complexes were washed and separated by SDS-PAGE. GST-PDZ bound Git1 (*top*) or β-Pix (*middle*) were identified by Western blotting using a GFP or HA antibody, respectively. *b,* NIH3T3 cells were treated with β-Pix or control siRNA oligonucleotides for 72 h. The cells were lysed and incubated (500 μg) with 10 μg of GST-SNX27 PDZ. The presence of bound β-Pix SNX27 (*middle*) and Git2 (*top*) were detected by Western blotting using the respective antibodies. 50 μg of cell lysate was run as input control. Equal staining was verified with Coomassie staining (*bottom*). *c,* NIH3T3 cells were treated with β-Pix or control siRNA oligonucleotides for 72 h. The cells were lysed and incubated (1 mg) with a SNX27 polyclonal antibody (5 μl). Immune complexes were collected using protein A-Sepharose. The presence of immunoprecipitated SNX27 (*bottom*), immunocomplex bound β-Pix (*middle*), or Git2 (*top*) were detected by Western blotting using the respective antibodies. 50 μg of cell lysate was run as input control. *MW*, molecular weight marker.

NIH3T3 cells (Fig. 5*c*). Control or β-Pix siRNA sequences were transfected into NIH3T3 cells, and 72 h post-transfection, the cells were lysed and incubated with GST·PDZ (Fig. 5*b*) or immunoprecipitated with SNX27 (Fig. 5*c*). At this time point the levels of β-Pix were routinely suppressed by over 70% (Fig. 5, *b, lower*, and *c*, *middle*), whereas Git2 protein levels were unaffected (Fig. 5, *b* and *c*). The amount of GST·PDZ-bound Git2 in cell lysates treated with β-Pix siRNA was severely diminished compared with control siRNA lysates (Fig. 5*b*). In

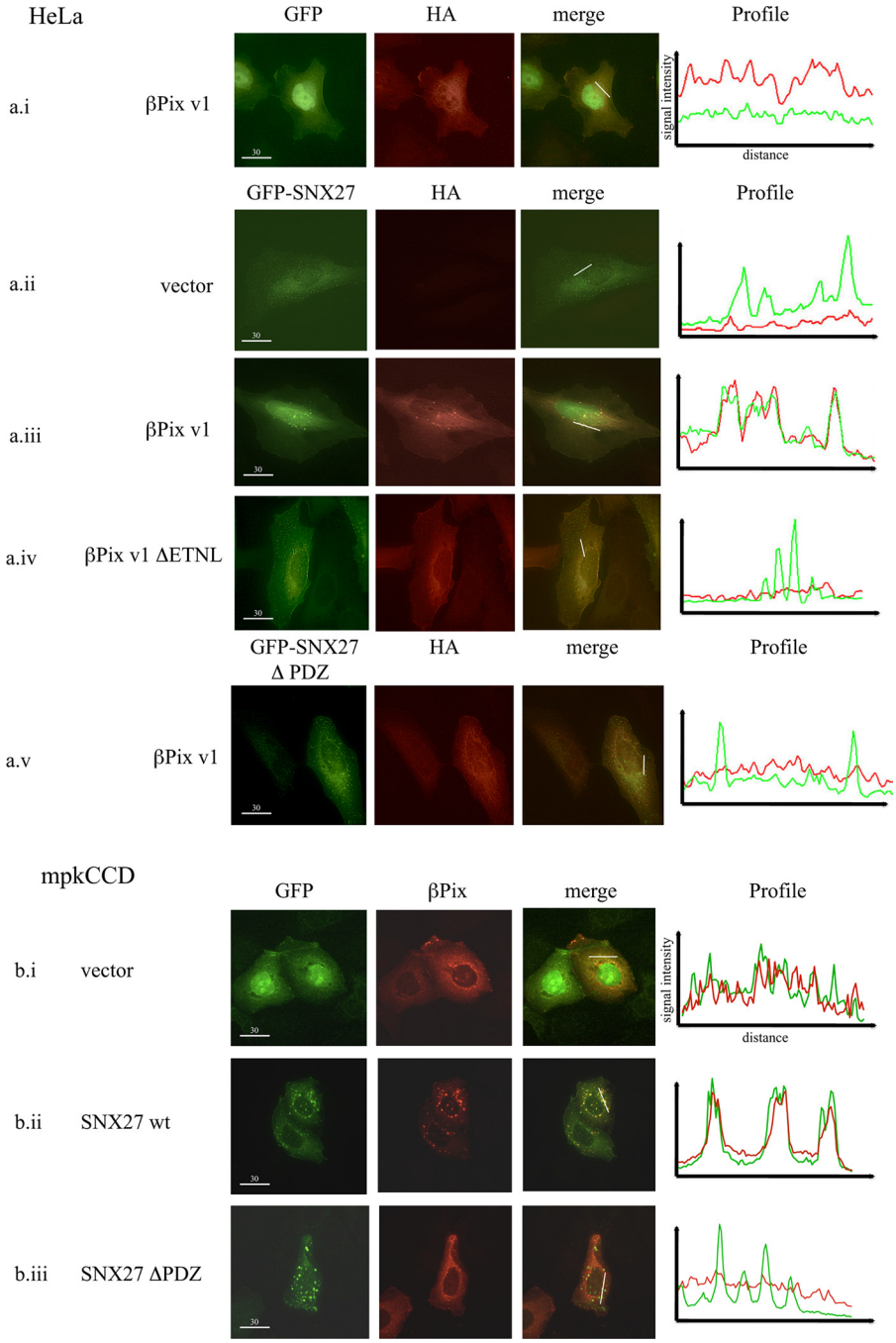

FIGURE 6. **SNX27 and β-Pix co-localize in endosomal sites.** *a*, HeLa cells were co-transfected with the indicated GFP-SNX27 or HA-β-Pix fusion proteins. After 24 h, the cells were fixed and permeabilized as described under "Experimental Procedures." β-Pix-expressing cells were identified by staining with an HA-specific antibody followed by an Alexa Fluor 594-nm conjugated secondary antibody. SNX27-expressing cells were identified by GFP. *b*, mpkCCD cells were co-transfected with the indicated GFP-SNX27 or mCherry-β-Pix fusion proteins. After 24 h the cells were fixed, and transfected cells visualized by GFP and mCherry, respectively. *Scale bar*, 30 μm.

addition, SNX27-complexed Git2 was only detected in immunoprecipitates from control siRNA-treated cell lysates (Fig. 5*c*). Taken together, the data suggest that the binding of Git with SNX27 is indirect and is mediated by β-Pix.

We then examined the subcellular localization of expressed SNX27 and β-Pix variants. Previous data have demonstrated that SNX27 is localized to the early endosome, whereas expressed β-Pix was observed at the leading edge of migrating cells, in membrane ruffles, and at focal adhesions (9, 28–30). Thus we postulated that SNX27 might be involved in the transient recruitment of β-Pix to endosomal sites or that β-Pix may regulate recruitment of SNX27 to the leading edge of migrating cells. To test these hypotheses, a series of GFP-tagged SNX27 and HA-tagged β-Pix plasmids were co-expressed in HeLa (*a*) and mpkCCD (*b*) cells (Fig. 6). Twenty-four hours post-transfection the cells were fixed and stained with an HA monoclonal antibody to mark β-Pix-transfected cells. Cells containing expressed SNX27 were visualized by GFP. Expressed β-Pix variant 1 in GFP control cells had a largely diffuse cytoplasmic localization, whereas the localization of GFP-SNX27 in HA

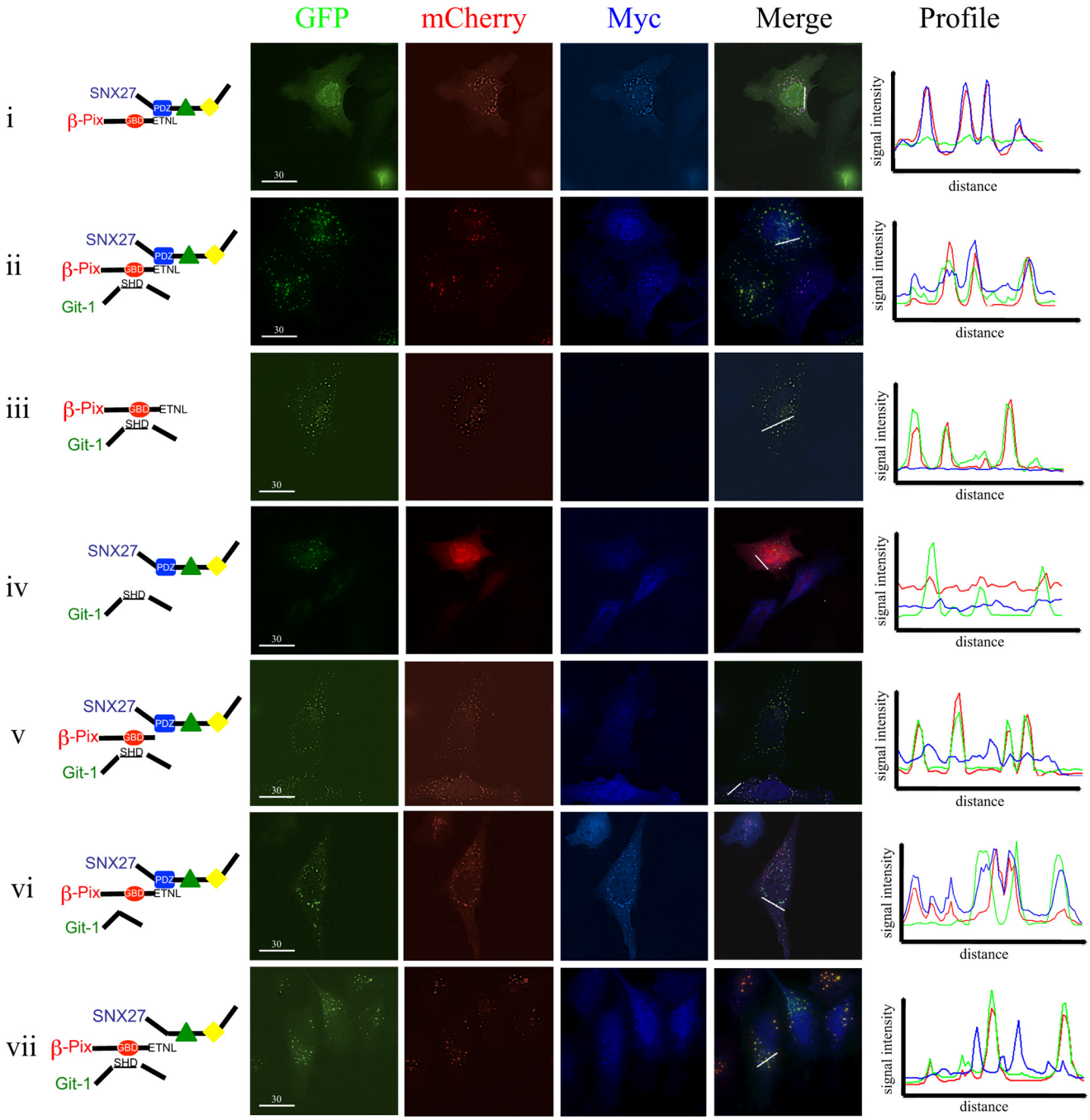

FIGURE 7. **The SNX27·β-Pix·Git tripartite complex co-localize in endosomal sites.** HeLa cells were co-transfected with the indicated GFP-Git, mCherry-β-Pix, and Myc-SNX27 fusion constructs. After 24 h, the cells were fixed and permeabilized as described under "Experimental Procedures." SNX27 expressing cells were identified by staining with a Myc-specific antibody, followed by an Alexa Fluor 647-nm conjugated secondary antibody. Git expressing cells were identified by GFP; β-Pix cells by mCherry. *Scale bar*, 30 μm.

control cells was predominantly vesicular as expected (Fig. 6*a*, *i* and *ii*). However, co-expression of GFP-SNX27 with HA-β-Pix variant 1 led to the redistribution of β-Pix variant 1 to endosomal sites overlapping the distribution of SNX27 (Fig. 6*a*, *iii*). Furthermore, in cells where β-Pix variant 1 and SNX27 were co-expressed, enlargement of endosomal sites were often noted (Fig. 6*a*, *iii*). The co-localization between β-Pix variant 1 and SNX27 in endosomal sites was abolished in cells where the β-Pix-SNX27 interaction is prevented (Fig. 6*a*, *iv* and *v*). SNX27-dependent recruitment of β-Pix to endosomal sites was also observed in mpkCCD cells (Fig. 6*b*). In conclusion, at least in an overexpression model, the interaction of SNX27 with β-Pix variant 1 may regulate recruitment of β-Pix variant 1 to components of the endocytic trafficking system.

Previous studies have localized Git proteins to endosomal sites (21, 22). Moreover, β-Pix has been shown to regulate the cellular localization of Git to large intracellular punctate structures (31). In this article, the authors also proposed the involvement of β-Pix C-terminal leucine zipper sequences in Git1 recruitment to these structures (31). However, the possibility

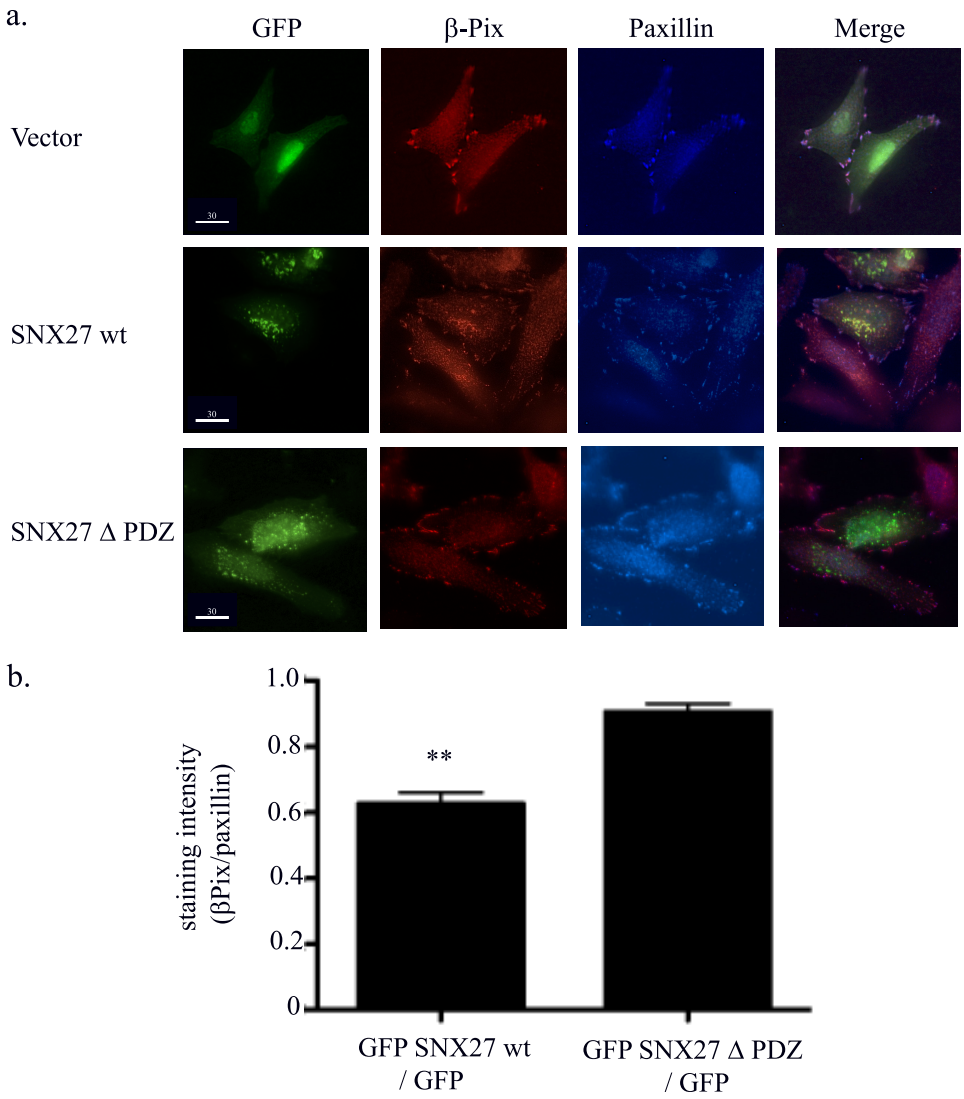

FIGURE 8. **SNX27-mediated movement of β-Pix from focal adhesions to the early endosome.** *a,* the indicated GFP-tagged SNX27 plasmids were transfected into HeLa cells. Twenty-four hours post-transfection the cells were fixed, permeabilized, and immunostained with β-Pix and paxillin, followed by rabbit Alexa Fluor-conjugated 568 nm and mouse Alexa Fluor 647 nm, respectively. SNX27-transfected cells were visualized by GFP. *Scale bar*, 30 μm. *b*, TIRF microscopy was used to measure the average density of β-Pix within focal adhesions. Using paxillin as a focal adhesion marker, the relative staining intensity of β-Pix was measured. The histogram represents one experiment measuring the ratio of β-Pix in focal adhesions in 7 GFP-SNX27 wild type or GFP-SNX27 ΔPDZ expressing cells to GFP control cells. The experiment was repeated three times with similar results (*, $p < 0.05$).

remained that the β-Pix-ETNL sequence might also be involved. Hence, we postulated that a SNX27·β-Pix complex could modulate the subcellular distribution of Git proteins (Fig. 7).

To this end, a series of GFP-tagged Git, mCherry-tagged β-Pix, and Myc-tagged SNX27 plasmids were expressed in HeLa cells. Twenty-four hours post-transfection, the cells were fixed and stained for Myc to mark SNX27-transfected cells (Fig. 7). GFP and mCherry enabled Git and β-Pix, respectively, to be visualized (Fig. 7). Co-localization of full-length β-Pix and SNX27 or full-length β-Pix and Git1 to vesicular structures was observed (Fig. 7, *i* and *iii*). In contrast, when full-length Git and SNX27 were co-expressed, both proteins were observed in vesicular structures, which did not overlap (Fig. 7, *iv*). When full-length Git, SNX27, and β-Pix were co-expressed, many vesicles appeared to contain two of the three expressed proteins with the third protein residing in a different vesicular site. However, there were many examples where localization of all three proteins did appear to overlap in the same cytoplasmic vesicle (Fig. 7, *ii*). To summarize, in the absence of β-Pix, SNX27 and Git may localize to distinct vesicular structures. When β-Pix is present, the three proteins may form a tripartite complex and occupy the same vesicular location.

We also tested whether the domains required for formation of the SNX27·β-Pix·Git complex *in vitro* were also required for co-localization *in vivo* (Fig. 7). First, expression of full-length Git1 and SNX27 with β-PixΔENTL led to a tight co-localization of β-Pix with Git in vesicular structures separate to SNX27 (Fig. 7*v*). Second, a similar observation was noted when full-length Git1 and β-Pix were co-expressed with SNX27 ΔPDZ (Fig. 7*vii*). Finally, co-localization of SNX27 with β-Pix in the early endosome was observed in cells where GitΔSHD, defective for β-Pix binding is co-expressed (Fig. 7*vi*). In conclusion, both biochemi-

cal and *in vivo* data presented here are in agreement of the existence of a SNX27·β-Pix·Git tripartite complex.

Endogenous β-Pix is readily observed in focal adhesions. To test whether SNX27 could redistribute endogenous β-Pix from these sites, we expressed GFP-tagged SNX27, SNX27ΔPDZ, or GFP alone in HeLa cells (Fig. 8*a*). After 48 h the cells were fixed and stained with a β-Pix polyclonal antibody and a paxillin monoclonal antibody to mark the focal adhesions (Fig. 8*a*). HeLa cells expressing GFP-SNX27 exhibited a clear redistribution of endogenous β-Pix from focal contacts to endosomal sites (Fig. 8*a, middle row*). Localization of paxillin was unaffected in GFP-SNX27 expressing cells (Fig. 8*a, middle row*). In contrast, redistribution of β-Pix to endosomal sites was not apparent in GFP-SNX27 ΔPDZ or GFP control cells.

Quantification of the SNX27-mediated redistribution of β-Pix was performed by TIRF microscopy (Fig. 8*b*). Using paxillin as a marker, the average intensity of β-Pix at paxillin-positive focal adhesions was quantified. The staining intensity of β-Pix at focal adhesions in cells expressing GFP-SNX27 and GFP-SNX27 ΔPDZ was quantified and illustrated graphically as a ratio with staining intensity in GFP controls (Fig. 8*B*). The results indicated that elevated levels of SNX27 led to an approximate 37% decrease of β-Pix at focal adhesions ($p < 0.05$). Thus, SNX27 may facilitate the trafficking of β-Pix away from focal adhesions.

β-Pix has been shown to regulate cell motility, perhaps via distribution of Git proteins (23, 28, 31). Hence, we postulated that if SNX27 was involved in β-Pix trafficking during cell motility, then the absence of SNX27 could restrict the intracellular movement of β-Pix to focal adhesions, leading to defects in migration. We generated an inducible lentiviral-mediated shRNA expression system to suppress the levels of SNX27 in HeLa (Fig. 9*a*, *i*) and mpkCCD cells (Fig. 9*a*, *ii*). Puromycin-resistant clones were treated with doxycycline to induce shRNA expression. Expression of the red fluorescent protein marker indicative of shRNA expression could be detected 48 h post-induction; at this point a small amount of SNX27 remained (data not shown). However, after 72 h treatment, the expression level of SNX27 was below the threshold of detection (Fig. 9*a*, *i*) and could be maintained for several weeks. Identical results were observed when a stable mouse mpkCCD cell line expressing SNX27 shRNA clone 5 was generated (Fig. 9*a*, *ii*).

The influence of SNX27 on β-Pix localization at focal adhesions prompted investigations on the effect of SNX27 depletion on the migration ability of HeLa and mpkCCD cells. In both cell lines, wound-healing assays revealed that SNX27 knockdown cells migrated more slowly than control cells (Fig. 9*b*, *i* and *ii*). During these assays, it was apparent that HeLa-SNX27 knockdown cells proliferated more slowly with apparent prolonged mitoses. However, over a 12-h period, the velocity of non-mitosing HeLa and mpkCCD cells were measured (Fig. 9*b*, *i* and *ii*). The velocity of control shRNA expressing HeLa and mpkCCD cells was consistently greater than SNX27 knockdown cells ($p < 0.0001$ and $p < 0.005$). Hence, SNX27-mediated defects in β-Pix trafficking can modulate epithelial cell migration.

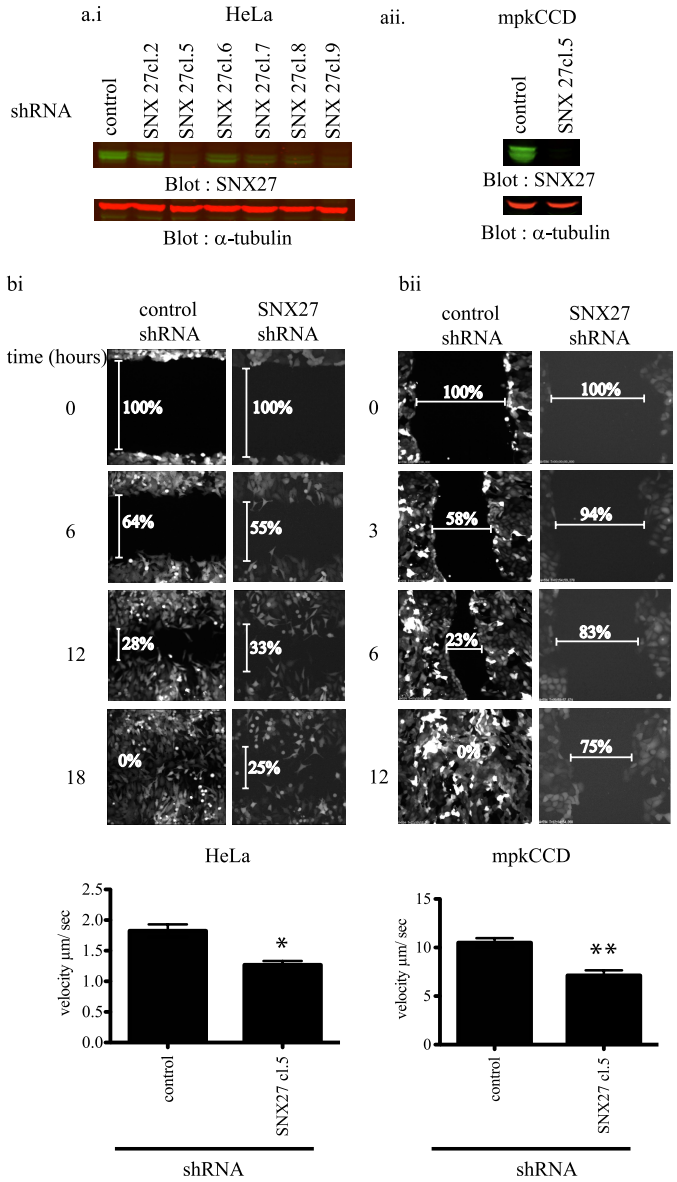

FIGURE 9. **SNX27 is required for HeLa and mpkCCD cell migration.** *a*, HeLa (*i*) and mpkCCD (*ii*) cells were infected with a panel of lentiviral SNX27 or control shRNA and selected with puromycin. shRNA expression was induced with 1 μg/ml of doxycycline for 72 h. At this time point, the cells were lysed and expression of SNX27 assessed by Western blotting (*top*). Equal loading was confirmed by Western blotting using an anti-α-tubulin antibody. *b*, control and SNX27 knockdown (shRNA#5) cells were cultured to confluence, the wound was created with pipette tip scraping and photographed at the indicated time points. Photographs were taken at 594 nm to mark shRNA expressing cells. Data shown are representative of three independent experiments. Six HeLa (*b*, *i*) or three mpkCCD (*b, ii*) cells per experiment at the edge of the scraped wound were individually tracked and the velocity (μm/s) of each was calculated over at least a 12-h period. The histograms represent the mean velocity; the *error bars* represent ± S.E. (in μm/s) of all cells measured. SNX27 knockdown cells migrate significantly slower than controls (*, $p < 0.0001$; **, $p < 0.003$; two-tailed *t* test).

DISCUSSION

The endocytic system consists of a series of distinct intracellular compartments involved in the sorting, processing, and breakdown of internalized protein cargo. Increasing evidence has revealed involvement of this system in such diverse cellular processes such as cytokinesis, cell polarity, and cell migration (1). Here, we propose the involvement of SNX27 as a key endo-

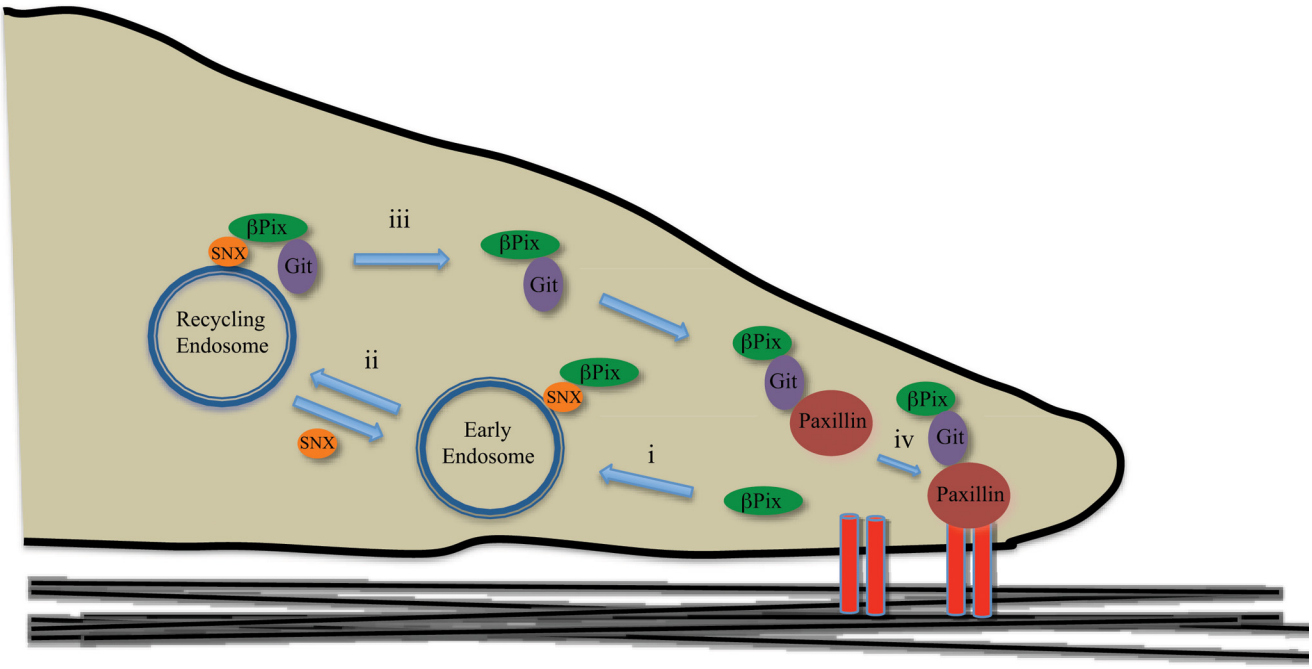

FIGURE 10. **Model for the role of SNX27 in trafficking of β-Pix between the endosomal compartment and focal contact sites.** Upon cell detachment from the extracellular matrix, β-Pix exits focal adhesion sites and translocates to the early endosome where interaction with SNX27 takes place (*i*). Transition of the early to recycling endosome facilitates formation of the tripartite SNX27·β-Pix·Git complex (*ii*). Upon cell adhesion, the β-Pix·Git complex is recycled to focal adhesions (*iii*) in complex with paxillin (*iv*).

somal component in the trafficking of β-Pix between the early endosome and focal contact sites.

Discovery of a Novel SNX27·β-Pix·Git1/2 Tripartite Complex—In a screen for novel SNX27 interacting proteins we identified robust interactions of SNX27 with β-Pix and both members of the Git family, Git1 and Git2. Using GST pulldown and co-immunoprecipitation techniques we demonstrated that the direct interaction between SNX27 and β-Pix is mediated by the PDZ domain of SNX27 and the type I PDZ binding motif of β-Pix. This conclusion is confirmed by the finding that of the known variants of β-Pix, β-Pix variant 1 (β1-Pix), which contains the carboxyl-terminal PDZ binding motif (ETNL) interacts with SNX27. β-Pix variant 3 (β2-Pix), which lacks the PDZ binding motif, does not (26). Hence, β-Pix may now be included in a growing list of SNX27-PDZ interaction proteins, which also include ion channels, receptors, and cytosolic proteins (7–11). SNX27 is the second protein identified to complex to the PDZ binding motif of β-Pix. The first, hScrib, was identified in a complex with β-Pix·Git, the ARF6 small GTPase, and the thyrotropin receptor (32, 33). Like SNX27, hScrib is known to interact with the β-Pix type I PDZ binding motif. The hScrib-β-Pix interaction was shown to regulate intracellular trafficking of the thyrotropin receptor with active Git and ARF6 also contributing to receptor recycling (33).

Both Git1 and Git2 lack C-terminal type 1 PDZ binding motifs. We mapped the Git region involved in SNX27 binding to the SHD and putative second coiled-coil domain (18). Notably, previous reports have indicated that these two Git domains are also important in β-Pix binding (15, 18). Hence, we proposed that SNX27, β-Pix, and Git could be part of a tripartite complex anchored by a central β-Pix molecule. This proposed interaction scheme is supported by several observations. First, the amount of Git co-precipitated in GST·PDZ complexes was dramatically elevated by co-expression of wild type β-Pix variant 1, but not by a form of variant 1 lacking the PDZ-binding motif. Second, siRNA directed against β-Pix severely diminished the amount of Git2 complexed to SNX27, determined by either GST pulldown or co-immunoprecipitation. Third, β-Pix induced co-localization of Git and SNX27.

Similar multipartite β-Pix·Git protein complexes are known to exist, and have been shown to participate in various cellular functions (34–37). For example, a proteomic approach identified myosin MYO18A as a binding partner to PAK2 (34). Similar to data presented in this article, the interaction between MYO18A and PAK2 was found to be indirect, and mediated by β-Pix·Git (34). Cells depleted of MYO18A displayed an increase in the number and size of focal adhesions, with concomitant decreased cell motility (34). A role in cell migration and/or cell spreading has also been proposed for a complex of β-Pix·Git with phospholipase Cγ1 and β-Pix·Git with paxillin and Crk (35, 36). Clearly, large multiprotein complexes containing β-Pix·Git may be involved in diverse cellular processes ranging from cell migration and vesicular trafficking.

Cellular Localization of the Complex—Numerous studies have localized β-Pix to focal contact sites and peripheral membranes (12, 13, 37). Overexpressed variant 1, found here to interact with SNX27, is the predominant variant in HeLa and NIH3T3 cells and was found to localize to the cell periphery and induce membrane ruffling. In contrast, variant 3, the dominant species in brain and the variant incapable of binding to SNX27, does not (26). We report here the first observation of β-Pix localization to endosomal structures. This localization of β-Pix is dependent on its interaction with the PDZ domain of SNX27.

The internalization and trafficking of β-Pix from focal adhesions is not surprising. Several reports have described trafficking of integrins and other focal adhesion components during cell motility and cytokinesis (38–40). Moreover, components of the clathrin-dependent endocytic apparatus have been detected in focal adhesions (39–41).

Git1 and Git2 have also been observed in focal adhesions and Rab11 positive recycling endosomes (22). In cells overexpressing SNX27, no difference in endogenous Git localization was apparent (data not shown). When SNX27 and Git were co-expressed, both proteins localized in endocytic vesicles but there was no evidence of co-localization. In contrast, co-expression of β-Pix with SNX27 and Git led to co-localization of all three proteins in an endocytic compartment.

SNX27-β-Pix-Git Interactions in Cell Motility—The biochemical interactions between SNX27, β-Pix, and Git coupled with the distinct cellular localizations of SNX27 and Git in the endocytic pathway suggest a model for β-Pix trafficking in the cell, which we propose may occur during cell motility (Fig. 10). Here, upon focal adhesion disassembly β-Pix is released. β-Pix is delivered to the early endosome, probably via a clathrin-dependent process (Fig. 10*i*). Here, β-Pix binds SNX27. The transition of the SNX27-containing early endosome to the recycling endosome leads to a transient Git-β-Pix-SNX27 interaction (Fig. 10*ii*). Eventually, β-Pix, in complex with Git, is delivered back to the plasma membrane from this recycling compartment (Fig. 10*iii*), in complex with paxillin (*iv*) (14, 21, 22). The identity of Rab GTPases members that might be responsible for trafficking of β-Pix between endocytic compartments is the subject of a future investigation.

Loss of SNX27 Decreases Cell Motility—Appropriate regulation of focal adhesion formation/maturation/disassembly is required for maintaining cell migration. Previous research has indicated that the endocytic trafficking system plays a key role in focal adhesion disassembly. In support of this, the observed recruitment of β-Pix to endosomes by SNX27 presented here suggests that SNX27 might influence focal adhesion stability and hence cell motility. We show that depletion of SNX27 from HeLa cells decreases cell motility. Although the mechanism by which SNX27 regulates cell motility may be β-Pix independent, we believe that the robust SNX27-β-Pix interaction observed here, along with numerous studies linking β-Pix with cell motility, is strong evidence that the regulation of SNX27-mediated cell motility may involve β-Pix.

The β-Pix·Git complex is also involved in recruitment of PAK to focal adhesions (12, 42). The amino-terminal of β-Pix binds PAK and strongly stimulates its activity (43). Furthermore, the effect of β-Pix·Git on cell migration has been proposed to be mediated by the targeting of activated PAK to adhesion sites (42). Preliminary data in our lab have identified activated PAK in complex with the tripartite SNX27·β-Pix·Git (data not shown). We have also observed activated PAK in the early endosome upon co-expression of SNX27 and β-Pix (data not shown). Hence, PAK may also be recycled to focal adhesions, also in a complex with β-Pix.

In conclusion, our data has added complexity to the mechanism by which the β-Pix·Git complex may regulate cell motility. Our data and data from other groups implicate SNX27 in cell proliferation and motility; two known cell characteristics deregulated in neoplasia (44). Hence, inhibition of SNX27 function may be important therapeutically.

Acknowledgments—We thank Julie Meeks, Richard Casady, and Brian Duchez for experimental contributions during this project, Angel Aponte for mass spectrometry expertise (NHLBI, NIH), and Guang Hu (NIEHS, NIH) for the donation of pINDUCER10 along with useful discussions. We also thank Dr. Patricia Sokolove for critically reading this manuscript. Finally, we are grateful to Wanjin Hong (Institute of Molecular and Cell Biology, Singapore) for the kind donation of a SNX27 polyclonal antibody and plasmid DNA at the beginning of our work with SNX27.

REFERENCES

1. Gould, G. W., and Lippincott-Schwartz, J. (2009) *Nat. Rev. Mol. Cell Biol.* **10,** 287–292
2. Palamidessi, A., Frittoli, E., Garré, M., Faretta, M., Mione, M., Testa, I., Diaspro, A., Lanzetti, L., Scita, G., and Di Fiore, P. P. (2008) *Cell* **134,** 135–147
3. Cullen, P. J. (2008) *Nat. Rev. Mol. Cell Biol.* **9,** 574–582
4. Worby, C. A., and Dixon, J. E. (2002) *Nat. Rev. Mol. Cell Biol.* **3,** 919–931
5. Kajii, Y., Muraoka, S., Hiraoka, S., Fujiyama, K., Umino, A., and Nishikawa, T. (2003) *Mol. Psychiatry* **8,** 434–444
6. Lee, H. J., and Zheng, J. J. (2010) *Cell Commun. Signal.* **8,** 8
7. Lauffer, B. E., Melero, C., Temkin, P., Lei, C., Hong, W., Kortemme, T., and von Zastrow, M. (2010) *J. Cell Biol.* **190,** 565–574
8. Rincón, E., Santos, T., Avila-Flores, A., Albar, J. P., Lalioti, V., Lei, C., Hong, W., and Mérida, I. (2007) *Mol. Cell. Proteomics* **6,** 1073–1087
9. Lunn, M. L., Nassirpour, R., Arrabit, C., Tan, J., McLeod, I., Arias, C. M., Sawchenko, P. E., Yates, J. R., 3rd, and Slesinger, P. A. (2007) *Nat. Neurosci.* **10,** 1249–1259
10. Joubert, L., Hanson, B., Barthet, G., Sebben, M., Claeysen, S., Hong, W., Marin, P., Dumuis, A., and Bockaert, J. (2004) *J. Cell Sci.* **117,** 5367–5379
11. MacNeil, A. J., Mansour, M., and Pohajdak, B. (2007) *Biochem. Biophys. Res. Commun.* **359,** 848–853
12. Manser, E., Loo, T. H., Koh, C. G., Zhao, Z. S., Chen, X. Q., Tan, L., Tan, I., Leung, T., and Lim, L. (1998) *Mol. Cell* **1,** 183–192
13. ten Klooster, J. P., Jaffer, Z. M., Chernoff, J., and Hordijk, P. L. (2006) *J. Cell Biol.* **172,** 759–769
14. Hoefen, R. J., and Berk, B. C. (2006) *J. Cell Sci.* **119,** 1469–1475
15. Loo, T. H., Ng, Y. W., Lim, L., and Manser, E. (2004) *Mol. Cell Biol.* **24,** 3849–3859
16. Turner, C. E., Brown, M. C., Perrotta, J. A., Riedy, M. C., Nikolopoulos, S. N., McDonald, A. R., Bagrodia, S., Thomas, S., and Leventhal, P. S. (1999) *J. Cell Biol.* **145,** 851–863
17. Botrugno, O. A., Paris, S., Za, L., Gualdoni, S., Cattaneo, A., Bachi, A., and de Curtis, I. (2006) *Eur. J. Cell Biol.* **85,** 35–46
18. Premont, R. T., Perry, S. J., Schmalzigaug, R., Roseman, J. T., Xing, Y., and Claing, A. (2004) *Cell Signal.* **16,** 1001–1011
19. Schlenker, O., and Rittinger, K. (2009) *J. Mol. Biol.* **386,** 280–289
20. Feng, Q., Baird, D., Yoo, S., Antonyak, M., and Cerione, R. A. (2010) *J. Biol. Chem.* **285,** 18806–18816
21. Di Cesare, A., Paris, S., Albertinazzi, C., Dariozzi, S., Andersen, J., Mann, M., Longhi, R., and de Curtis, I. (2000) *Nat. Cell Biol.* **2,** 521–530
22. Matafora, V., Paris, S., Dariozzi, S., and de Curtis, I. (2001) *J. Cell Sci.* **114,** 4509–4520
23. Meerbrey, K. L., Hu, G., Kessler, J. D., Roarty, K., Li, M. Z., Fang, J. E., Herschkowitz, J. I., Burrows, A. E., Ciccia, A., Sun, T., Schmitt, E. M., Bernardi, R. J., Fu, X., Bland, C. S., Cooper, T. A., Schiff, R., Rosen, J. M., Westbrook, T. F., and Elledge, S. J. (2011) *Proc. Natl. Acad. Sci. U.S.A.* **108,** 3665–3670
24. Kuo, J. C., Han, X., Hsiao, C. T., Yates, J. R., 3rd, and Waterman, C. M. (2011) *Nat. Cell Biol.* **13,** 383–393
25. Jeleń, F., Oleksy, A., Smietana, K., and Otlewski, J. (2003) *Acta Biochim.*

Pol. **50,** 985–1017
26. Koh, C. G., Manser, E., Zhao, Z. S., Ng, C. P., and Lim, L. (2001) *J. Cell Sci.* **114,** 4239–4251
27. Frank, S. R., and Hansen, S. H. (2008) *Semin. Cell Dev. Biol.* **19,** 234–244
28. Campa, F., Machuy, N., Klein, A., and Rudel, T. (2006) *Cell Res.* **16,** 759–770
29. Lee, J., Jung, I. D., Chang, W. K., Park, C. G., Cho, D. Y., Shin, E. Y., Seo, D. W., Kim, Y. K., Lee, H. W., Han, J. W., and Lee, H. Y. (2005) *Exp. Cell Res.* **307,** 315–328
30. Lee, S. H., Eom, M., Lee, S. J., Kim, S., Park, H. J., and Park, D. (2001) *J. Biol. Chem.* **276,** 25066–25072
31. Za, L., Albertinazzi, C., Paris, S., Gagliani, M., Tacchetti, C., and de Curtis, I. (2006) *J. Cell Sci.* **119,** 2654–2666
32. Audebert, S., Navarro, C., Nourry, C., Chasserot-Golaz, S., Lécine, P., Bellaiche, Y., Dupont, J. L., Premont, R. T., Sempéré, C., Strub, J. M., Van Dorsselaer, A., Vitale, N., and Borg, J. P. (2004) *Curr. Biol.* **14,** 987–995
33. Lahuna, O., Quellari, M., Achard, C., Nola, S., Méduri, G., Navarro, C., Vitale, N., Borg, J. P., and Misrahi, M. (2005) *EMBO J.* **24,** 1364–1374
34. Hsu, R. M., Tsai, M. H., Hsieh, Y. J., Lyu, P. C., and Yu, J. S. (2010) *Mol. Biol. Cell* **21,** 287–301
35. Lamorte, L., Rodrigues, S., Sangwan, V., Turner, C. E., and Park, M. (2003) *Mol. Biol. Cell* **14,** 2818–2831
36. Jones, N. P., and Katan, M. (2007) *Mol. Cell. Biol.* **27,** 5790–5805
37. Liu, F., Jia, L., Thompson-Baine, A. M., Puglise, J. M., Ter Beest, M. B., and Zegers, M. M. (2010) *Mol. Cell. Biol.* **30,** 1971–1983
38. Pellinen, T., Tuomi, S., Arjonen, A., Wolf, M., Edgren, H., Meyer, H., Grosse, R., Kitzing, T., Rantala, J. K., Kallioniemi, O., Fässler, R., Kallio, M., and Ivaska, J. (2008) *Dev. Cell* **15,** 371–385
39. Chao, W. T., Ashcroft, F., Daquinag, A. C., Vadakkan, T., Wei, Z., Zhang, P., Dickinson, M. E., and Kunz, J. (2010) *Mol. Cell. Biol.* **30,** 4463–4479
40. Ezratty, E. J., Bertaux, C., Marcantonio, E. E., and Gundersen, G. G. (2009) *J. Cell Biol.* **187,** 733–747
41. Ezratty, E. J., Partridge, M. A., and Gundersen, G. G. (2005) *Nat. Cell Biol.* **7,** 581–590
42. Manabe, R., Kovalenko, M., Webb, D. J., and Horwitz, A. R. (2002) *J. Cell Sci.* **115,** 1497–1510
43. Bagrodia, S., Bailey, D., Lenard, Z., Hart, M., Guan, J. L., Premont, R. T., Taylor, S. J., and Cerione, R. A. (1999) *J. Biol. Chem.* **274,** 22393–22400
44. Cai, L., Loo, L. S., Atlashkin, V., Hanson, B. J., and Hong, W. (2011) *Mol. Cell Biol.* **31,** 1734–1747